## AD NUMBER

AD876697

## NEW LIMITATION CHANGE

TO

Approved for public release, distribution unlimited

FROM

Distribution: USGO: others to Director, Defense Atomic Support Agency, Washington, D. C. 20305.

## AUTHORITY

DTRA ltr, 3 Nov 99

DASA 2536
R-251

# FURTHER LABORATORY STUDIES OF THE PERTURBED UPPER ATMOSPHERE

**Final Report**

**Contract DASA 01-70-C-0032**

**September 1970**

**M. N. Hirsh and P. N. Eisner**



**THE DEWEY ELECTRONICS CORPORATION**
**11 Park Place, Paramus, N.J. 07652**

52

Further transmittal of this document outside the agencies of the U.S. Government must have prior approval of the Director, Defense Atomic Support Agency, Washington, D.C. 20305.

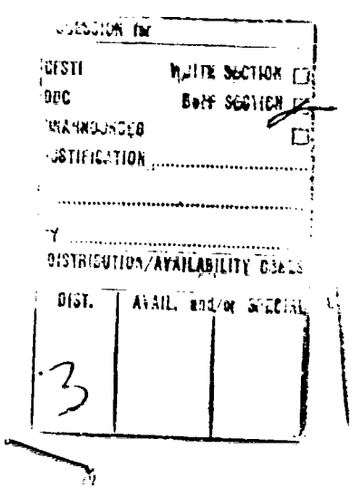

(1)

DASA 2536

FINAL REPORT R-251

SEPTEMBER, 1970

# FURTHER LABORATORY STUDIES OF THE PERTURBED UPPER ATMOSPHERE

by

M. N. HIRSH

P. N. EISNER

CONTRACT NO. DASA01-70-C-0032

This research has been sponsered by the Defense Atomic Support Agency under NWER Subtask HC010.



THE DEWEY ELECTRONICS CORPORATION

11 PARK PLACE

PARAMUS, NEW JERSEY 07652

## ABSTRACT

Laboratory studies have been made of the positive and negative ions resulting from the irradiation of airlike $N_2$:$O_2$ mixtures at total pressures between 1 and 8 Torr by megavolt electrons. For gas mixtures containing less than 1 ppm $H_2O$, only $O_2^+$ and $O_2^-$ are observed at the onset of irradiation; as the electron bombardment continues, these ions interact with beam-generated minority species to produce an ion spectrum eventually dominated by $NO^+$, $NO_2^-$, and $NO_3^-$. Quantitative studies of the removal of $O_2^+$ by charge-exchange with beam-generated NO yield for the dominant NO-producing mechanism the reaction

$$O_2^+ + N_2 \rightarrow NO^+ + NO,$$

with the rate coefficient $k=(1.0 \pm 0.25) \times 10^{-16}$ $cm^3/sec$. From the initial $O_2^+$ decays, an upper limit of $1.4 \times 10^{-7}$ $cm^3/sec$ is found to the coefficient for two-body ionic recombination of $O_2^+$ and $O_2^-$. If $H_2O$ concentrations between 5 and 20 ppm are added to the gas, the positive ion spectrum observed after long irradiation is dominated by complex ions of the form $H_3O^+.n\ H_2O (n=0, 1, 2, \ldots)$, in agreement with *in situ* observations in the D region. In the radiation afterglow, $H_3O^+$ and $H_3O^+.H_2O$ are lost by first-order reactions with apparent rate coefficients of $2.8 \times 10^{-28}$ $cm^6/sec$ and $3.6 \times 10^{-28}$ $cm^6/sec$, respectively to within a factor of 2. Except for a small increase in the $NO_3^-.H_2O$ peak, the negative ion spectrum is essentially unchanged by concentrations of up to 20 ppm $H_2O$.

## ACKNOWLEDGMENTS

The authors wish to express their gratitude to Elias Poss for his participation in the measurement program, and to David R. Maerz for his technical assistance. The importance of several discussions with Dr. Franklin A. Niles, of the Ballistics Research Laboratory, Aberdeen Proving Ground, Maryland, in the interpretation of the experimental results is gratefully acknowledged.

## TABLE OF CONTENTS

## LIST OF ILLUSTRATIONS

## I. INTRODUCTION

This report describes work performed under Contract No. DASA 01-70-C-0032, entitled, "Further Laboratory Study of the Perturbed Upper Atmosphere." The experimental work was performed by members of the staff of The Dewey Electronics Corporation's Space Physics Laboratory in New York City, as one of a continuing series of laboratory investigations of ionospheric chemistry initiated by the impact of relativistic electrons on air. The experiments consist of mass spectrometer studies of the ambient positive and negative ions in airlike mixtures of 80% $N_2$, 20% $O_2$, during and after electron irradiation, and to the effects of small added quantities of water vapor on the ion spectra in irradiated air.

Two publications by members of the laboratory staff and related to the subject program appeared in the literature during the period covered by this report. They are:

a) "A Laboratory Facility for Ionospheric Reaction Studies," M. N. Hirsh, P.N. Eisner, and J. A. Slevin, Rev. Sci. Inst. 39, 1547 (1968)

b) "Ionization and Attachment in $O_2$ and Airlike $N_2$:$O_2$ Mixtures," M. N. Hirsh, P. N. Eisner, and J. A. Slevin, Phys. Rev. 178, 175 (1969)

## II. Motivation For Present Work

Recent mass spectrometer measurements in the ionospheric D-region [Narcisi, 1967] reveal an ionic composition markedly different from the $O_2^+$, $O_2^-$ spectrum generally accepted only a few years ago. The existence and importance of $NO^+$, the hydronium sequence $H_3O^+ \cdot nH_2O$, and the atomic metal ions, at least above 60km, are now well established (lower altitudes are as yet outside the range of the mass spectrometer probes). The additional problem remains, however, of understanding the sequence of chemical events producing the observed ions, so that we can predict the effects of changes in external conditions on the ion spectra.

There are three promising approaches to the improvement of our knowledge in this respect. The first is the combination of reaction rate measurements and a computer code which solves simultaneously a set of reaction-rate equations based on these measurements, one for each time-varying ionic and neutral species of interest [Keneshea, 1962; Niles, 1970]; this approach may be considered a theoretical simulation of the ionosphere. The second approach involves systematic *in situ* measurements of ion and neutral species as a function of natural parameters (altitude, sunlight, auroral disturbances, *etc.*) The third approach is a laboratory simulation of the ionosphere itself, in which the neutral composition, physical conditions, and sources of excitation characteristic of the ionospheric process being studied are duplicated as closely as possible. Such a simulation combines the relevance of the *in situ* measurements with the convenience and degree of control of a laboratory experiment. Although a complete simulation of the entire ionospheric problem may be beyond technical and financial feasibility, an experiment which reproduces the essential features of some limited aspect of the ionospheric problem is useful [Hirsh, *et al.*, 1968; 1969; 1970].

This report presents the results of a series of such partial simulation experiments utilizing mass spectrometer measurements in airlike mixtures of 80% $N_2$, 20% $O_2$ irradiated by megavolt electrons, under controlled conditions which resemble those in the lower ionosphere; the measurements are thus well suited both for detailed comparison with the predictions of a chemistry code and for direct comparison with *in situ* measurements on the ionosphere. During prolonged high-energy electron bombardment, neutral species are formed in the airlike mixture which alter the ion spectrum; in this report we study in detail the buildup of one such species, NO, and its effect on the positive-ion spectrum. The negative-ion spectrum is also shown to be a function of irradiation time. We have also performed measurements of hydrated cluster ions in $N_2$:$O_2$ mixtures containing small quantities of water; those results are also presented and compared with the available ionospheric data. Since the experimental results are particularly pertinent to the altitude region below 50km, they should provide some useful guideposts to the understanding of the chemistry of the lower D region under both ambient and disturbed conditions.

## III. Description of the Experiment

The experimental system is shown schematically in Figure 1. The airlike $N_2$:$O_2$ mixture is placed into the large reaction chamber, where it is irradiated uniformly over its volume by a diffuse beam of monoenergetic electrons from the Van de Graaff accelerator, in the energy range 0.5 to 1.7 MeV. These electrons rapidly traverse the chamber, leaving a distribution of thermal electrons, ions, and excited neutral species in the gas. We study the subsequent behavior of this excited system, using various diagnostic techniques which are described below. The gas can be irradiated continuously with the electron beam, or the beam may be pulsed on and off repetitively, thus permitting both steady-state and transient measurements of selected gas properties to be made. From these measurements we can deduce both production and removal rates for the species of interest. The use of a large reaction chamber, 1.2 meters in diameter and 0.6 meter long, minimizes wall effects due to the release of occluded impurities and to the surface catalysis of chemical reactions. The combination of large chamber and spatially uniform electron beam completely filling it reduces the loss rates of particles by diffusion to the walls to negligible values, even at pressures as low as 1 Torr (simulated altitudes of 45 km). To reduce impurity effects even further, we employ ultrahigh-vacuum techniques in the preparation of the chamber for gas filling, including prolonged bakeout. A detailed description of the system appears in the literature [Hirsh et al., 1968].

We have used the system described above to study the production of electron-ion pairs in atmospheric gases by megavolt electrons, and the disappearance of thermal electrons by three-body attachment to $O_2$, under conditions closely resembling those in the ionosphere [Hirsh et al., 1969].

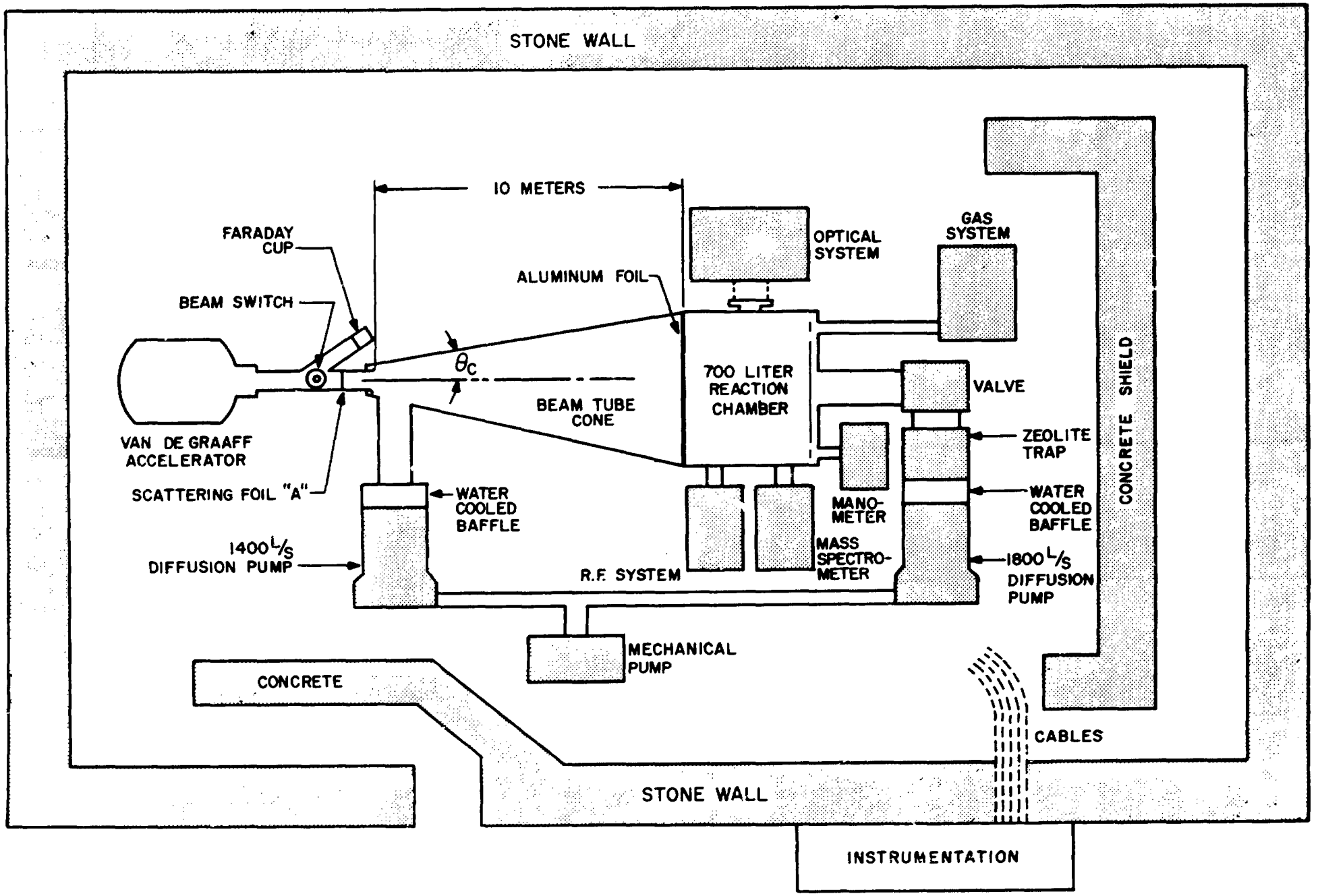


Figure 1. Schematic Diagram of Experimental System

We have also performed absolute intensity measurements on the fluorescent emission of the 3914-Å band of $N_2^+$, to determine the production of excited states during electron-impact ionization [Hirsh et al., 1970].

For the chemistry studies reported here, we have made mass spectrometer measurements of the ambient positive and negative ions formed in the irradiated gas. Ions have been studied in the steady state, as well as time-resolved in the pulsed-beam experiments. The mass spectrometer, a differentially-pumped rf monopole instrument, has an entrance aperture at the chamber wall, through which ions from the gas diffuse; the use of ion-extraction fields, which might distort the thermal chemistry in the ambient gas, is avoided. We have developed a model for the ion sampling which relates ion currents seen in the mass spectrometer to ion densities in the center of the chamber, away from the walls (cf. Appendix); the relationship for species i is:

$$J_i = G\sqrt{D_i \nu_i}\; n_i \qquad (1)$$

where $J_i$ is the observed ion current for the species, $D_i$ its diffusion coefficient, $\nu_i$ its total volume removal frequency, and $n_i$ its volume density near the center of the chamber. G is a constant which includes the aperture area, the transmission of the spectrometer, and the efficiency of the ion detector.

## IV. General Features of the Ion Spectra in Dry Air

In the present experiment, the chamber is filled with the airlike $N_2$:$O_2$ mixture (containing about 1 ppm impurities, about half of which is $H_2O$,) to a pressure between 1 and 10 Torr, and irradiated with the electron beam. At the start of the irradiation, in addition to the free thermal electrons in the gas, which we have described elsewhere [Hirsh et al., 1969], two ion species are seen in the mass spectrometer, $O_2^-$ and $O_2^+$. The observation of $O_2^-$ identifies it as the stable ion ultimately produced in the three-body attachment of thermal electrons of neutral $O_2$. All of the primary positive ions other than $O_2^+$ which can be produced by the passage of fast electrons through the $N_2$:$O_2$ mixture, i.e. $N_2^+$, $N^+$, and $O^+$, are known to undergo rapid charge exchange with $O_2$, so that only $O_2^+$ can be expected to be seen in the mass spectrometer during the first few seconds of irradiation [Niles, 1970].

If the fast-electron beam irradiation is terminated abruptly before the gas has been exposed to an appreciable amount of irradiation, the thermal electrons disappear within a few milli-seconds by three-body attachment. The $O_2^+$ and $O_2^-$ ions decay non-exponentially on a time scale of the order of one second by mutual ionic recombination; this process is outside the scope of this program, and will be described elsewhere.

If the continuous irradiation is again resumed, the $O_2^-$ and $O_2^+$ ions originally observed begin to decrease, to be replaced by signals from other ionic species, as illustrated schematically in Figure 2. After about 20 minutes of irradiation, a stable in-beam ion composition is attained, consisting primarily of $NO^+$, $NO_2^-$, and $NO_3^-$

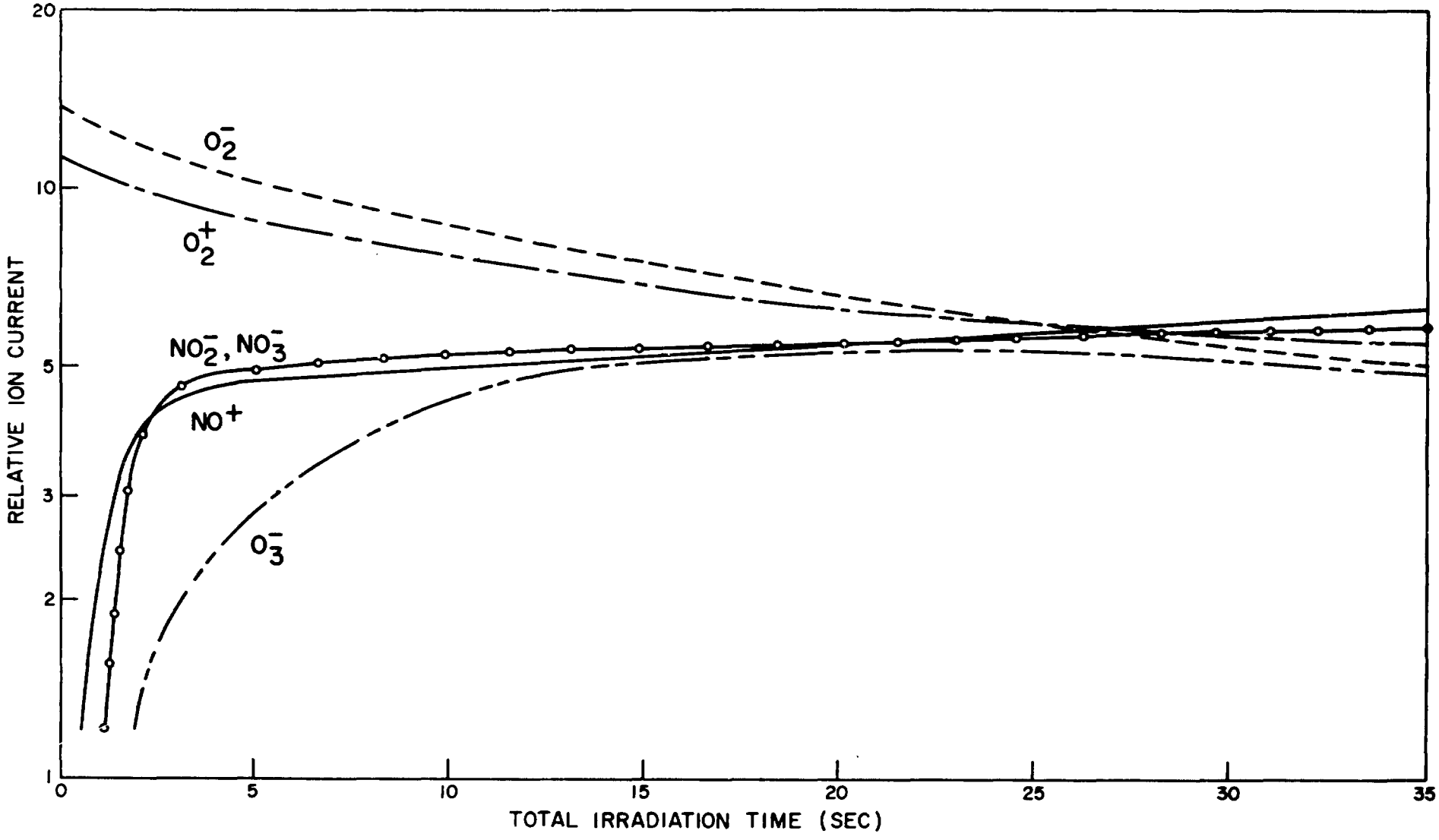


Figure 2. Variation of Observed Ion Currents with Total Accumulated Radiation Dose

with small amounts of $O_2^-$ and $O_2^+$; the observed ratio of the ion current from $NO_2^-$ to that from $NO_3^-$ decreases at higher gas pressures. If the initial gas mixture contains a few parts per million of $H_2O$, the entire ion spectrum is altered, as will be discussed below.

In the radiation afterglow in a gas mixture which has been subjected to this prolonged irradiation, the electrons again disappear within a few milliseconds by three-body attachment, at a rate apparently unaffected by chemical changes induced in the gas by the irradiation [Hirsh, et al., 1969]. $O_2^+$ and $O_2^-$ decay exponentially on a tens-of-milliseconds time scale, in contrast to the slower non-exponential decay which characterized those ions early in the irradiation history of the gas. The major ions in the irradiated gas, i.e., $NO^+$, $NO_2^-$, and $NO_3^-$, decay on a time scale of the order of one second by ionic recombination; of these three dominant species, $NO_2^-$, decays most rapidly.

## V. Buildup of NO in Dry Air During Prolonged Irradiation

### A. Experimental Observations

The replacement of $O_2^+$ by $NO^+$ as the dominant positive ion during continued irradiation is a striking feature of the radiation chemistry. To obtain detailed quantitative information on this process, we have performed the following series of experiments. With the mass spectrometer tuned to the $O_2^+$ peak, and a fresh sample of the $N_2$:$O_2$ mixture in the chamber, the electron beam is pulsed on and off repetitively with a low duty cycle; this permits observation of the $O_2^+$ afterglow decay without exposing the gas to significant amounts of radiation. The decay of ion current in the afterglow is recorded, after which the gas is irradiated for a fixed time interval with the beam operating continuously; the pulsed mode is then employed as before to determine the afterglow decay appropriate to the irradiated gas. An example of the afterglow decays obtained in this way for various radiation doses is shown in Figure 3. The decrease of the $O_2^+$ ion current is exponential over this range of experimental parameters; from the sampling theory, this implies that the central ion densities also decay exponentially, with the same characteristic time constants as the ion currents. It can be seen that increasing the time of irradiation results in an increased loss frequency for the ion. Figure 4 shows the results of a series of measurements of the $O_2^+$ loss frequency as a function of gas pressure and irradiation time; the results can be summarized by a loss frequency which varies as the first power of the gas pressure and as the square root of the total irradiation time; specifically,

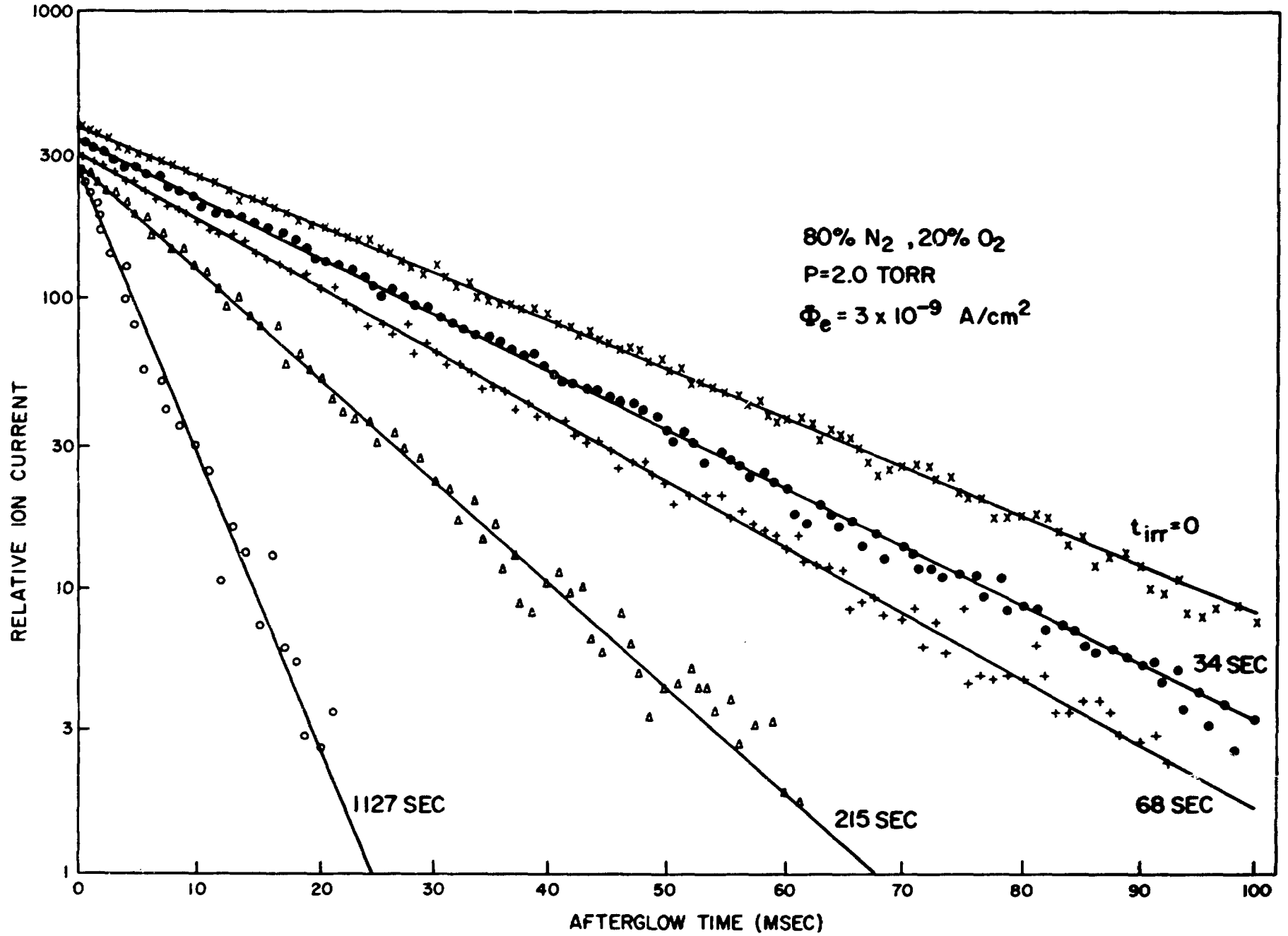


Figure 3. The Effect of Prior Irradiation on $O_2^+$ Decay Frequencies in the Radiation Afterglow

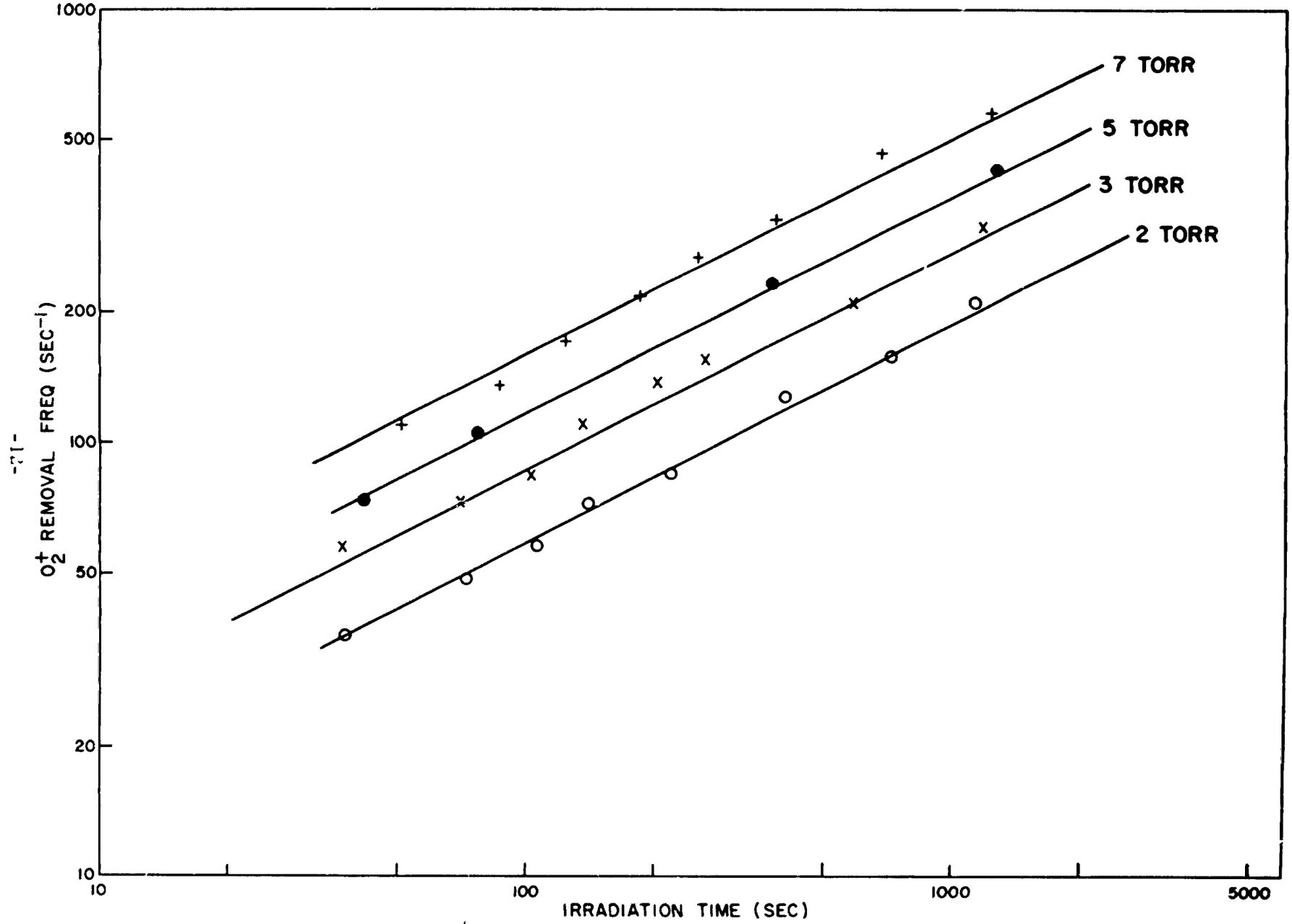


Figure 4. Variation of $O_2^+$ Removal Frequency with Irradiation Time and Gas Pressure

$$\nu_L(O_2^+) = (85 \pm 20)\, p\sqrt{it} \ \ sec^{-1},$$

where p is in Torr, i is in $\mu A/cm^2$ of 1.0 MeV electrons, and t is the irradiation time in seconds.

The in-beam $O_2^+$ density is the ratio of the production rate S to the loss frequency $\nu_L$. As the irradiation progresses, the $O_2^+$ density decreases as $\nu_L^{-1}$, so that from (1) the observed ion current is given by

$$J(O_2^+) = GS\sqrt{D/\nu_L} \propto t^{-1/4}. \qquad (2)$$

This behavior is illustrated in Figure 5. This observation corroborates both the ion sampling theory and the constancy of the source term S with irradiation.

Figure 6 shows the non-exponential afterglow decay of the $NO^+$ ion current obtained after the gas had been previously irradiated by the electron beam for 20 minutes. This decay mode, which is typical for $NO^+$ at all times during the radiation history, is related to the ionic recombination process rather than to the radiation chemistry itself and will not be discussed further here.

B. Interpretation of Experimental Results

The incident electron beam, in passing through the gas, produces ion-electron pairs at the rate [Hirsh, et al., 1969],

$$S = 4.93 \times 10^{11} \text{ pi } [\text{cm/sec Torr } \mu A]^{-1}. \qquad (3)$$

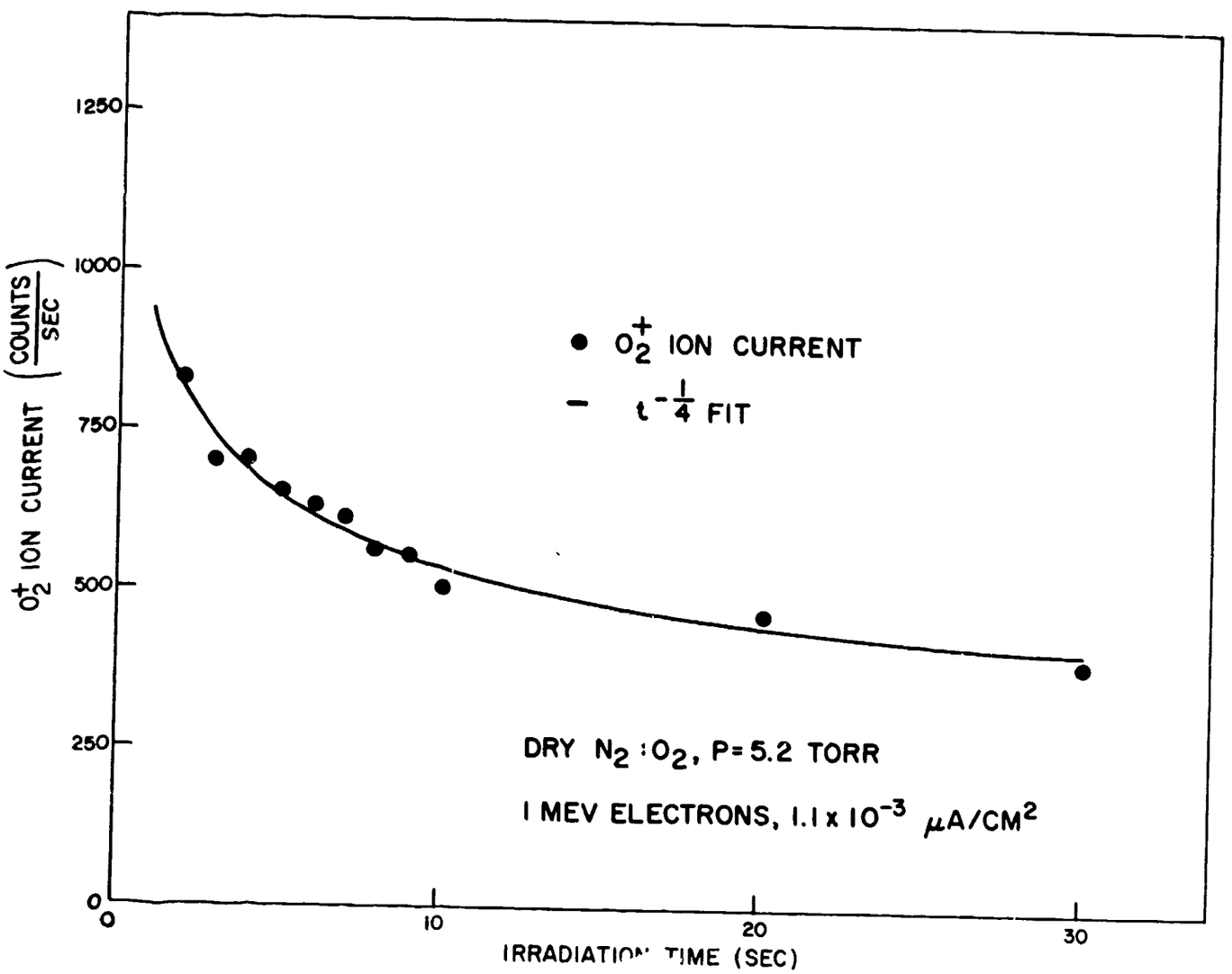


Figure 5. Comparison of Measured and Predicted Variation of $O_2^+$ In-Beam Ion Current with Irradiation Time

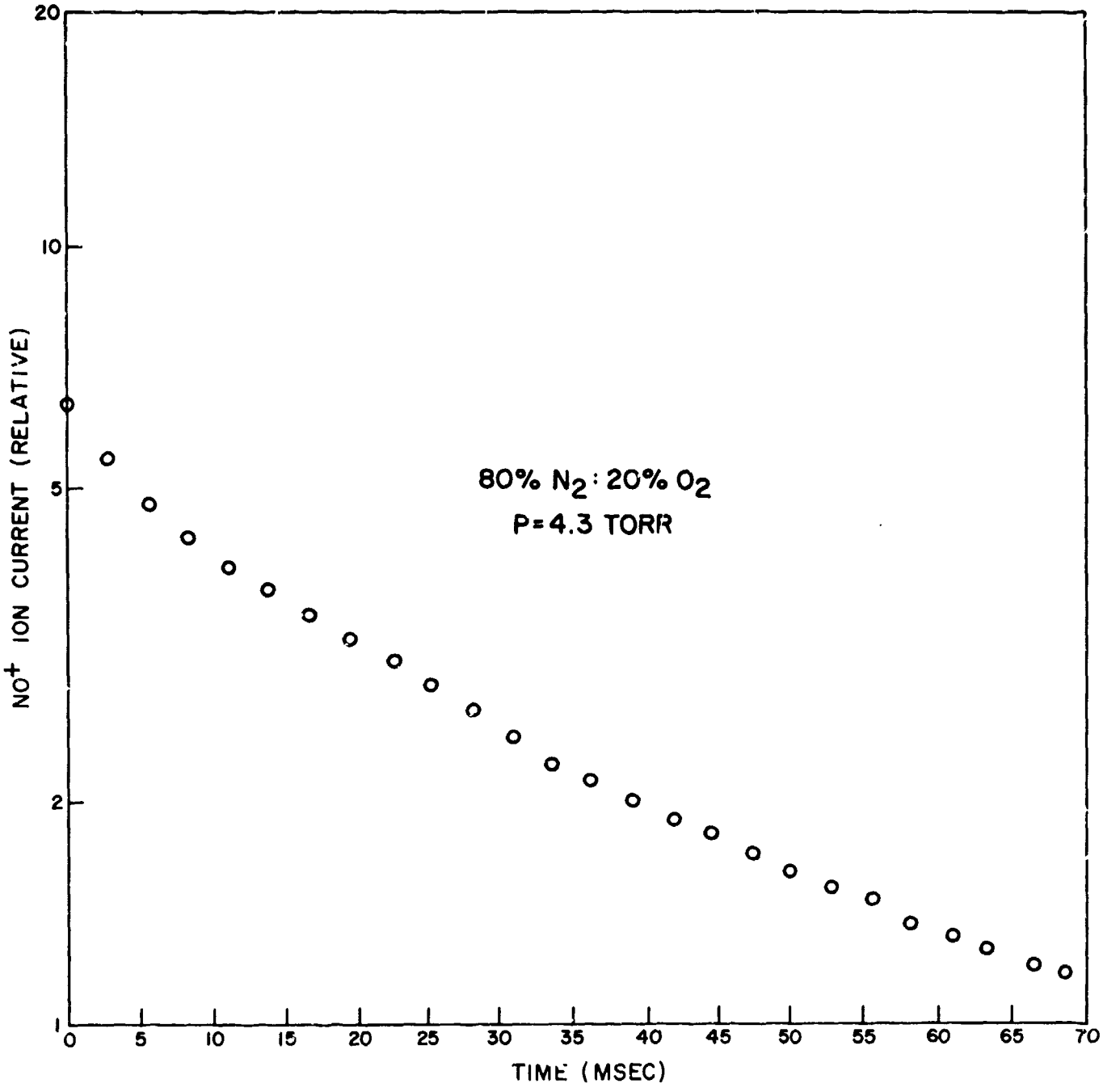


Figure 6. Recombination- Controlled Decay of $NO^+$ in the Afterglow

In view of the rapid charge transfer to $O_2$ mentioned above, (3) can be taken as the rate of production of $O_2^+$ ions.

Under the present conditions only three reactions should play a role in the disappearance of $O_2^+$ [Niles, 1970]:

(a) $O_2^+ + N_2 \rightarrow NO^+ + NO$ ; $k_1 = 1 \times 10^{-16} cm^3/sec$

(b) $O_2^+ + NO \rightarrow O_2 + NO^+$ ; $k_2 = 8 \times 10^{-10} cm^3/sec$

(c) $O_2^+ + M^- \rightarrow O_2 + M$ ; $\alpha_3 \simeq 1 \times 10^{-7} cm^3/sec$

We expect no other process to be able to remove $O_2^+$ at significant rates in this experiment. The ion-atom interchange reaction (a) provides a removal frequency for $O_2^+$ which is independent of irradiation time, since the $N_2$ density is not changed sensibly during the irradiation. The NO produced by this reaction, however, provides an irradiation-dependent decay frequency for $O_2^+$ through the charge exchange reaction (b). It will be seen below that the exact numerical value of the coefficient for recombination of $O_2^+$ with all ambient negative charge $M^-$ does not propagate into the solution for the radiation chemistry, and needs no further specification than that given above.

For completeness in specifying the NO density, we include the following cycle of reactions which involve the N atom; the importance of this cycle under the present experimental conditions is again suggested by the AIRCHEM computations [Niles, 1970]:

(d) $N + O_2 \rightarrow NO + O$ ; $k_4 = 8.6 \times 10^{-17} cm^3/sec$

(e) $N + NO \rightarrow N_2 + O$ ; $k_5 = 2.2 \times 10^{-11} cm^3/sec$

The N atom is produced by dissociative ionization of $N_2$ by the incident megavolt electrons; if a fraction $\zeta$ of all ionization events are dissociative, then the source term for N atoms is $\zeta S$. It has been estimated that $\zeta$ is of the order of 0.2 [Dalgarno, 1967]. We assume that reactions (d) and (e) dominate the N atom removal processes.

For completeness in the reaction sequence, we include the recombination of $NO^+$ with negative ions [Eisner and Hirsh, 1970];

$$(f)\quad NO^+ + M^- \rightarrow NO + M;\quad \alpha_6 \simeq 1 \times 10^{-7} cm^3/sec.$$

The remarks made above in connection with reaction (c) also apply to (f).

The sequence of reactions above can be expressed as reaction rate equations for each of the four time-varying species; in the following, square brackets denote the number density of the bracketed species.

$$\frac{d[O_2^+]}{dt} = S - k_1[N_2][O_2^+] - k_2[NO][O_2^+] - \alpha_3[M^-][O_2^+]. \qquad (4)$$

$$\frac{d[NO^+]}{dt} = k_1[N_2][O_2^+] + k_2[NO][O_2^+] - \alpha_6[M^-][NO^+]. \qquad (5)$$

$$\frac{d[N]}{dt} = \zeta S - k_4[O_2][N] - k_5[NO][N]. \qquad (6)$$

$$\frac{d[NO]}{dt} = k_1[N_2][O_2^+] + k_4[O_2][N] + \alpha_6[M^-][NO^+] - k_2[O_2^+][NO] - k_5[N][NO]. \qquad (7)$$

The time scales for changes in the $O_2^+$, $NO^+$, and N densities are comparable with the beam-pulsing time sequence; the density of NO changes slowly over many cycles of the beam pulsing. We may therefore solve Equations (4), (5), and (6) for quasi-steady solutions in which NO is treated as a slowly-changing parameter. Equation (4) yields immediately:

$$[O_2^+] = \frac{S}{k_1[N_2] + k_2[NO]} \qquad (8)$$

where we have taken advantage of the observed exponential decay of $O_2^+$ by neglecting a term $\alpha_1[M^-]$ in the denominator of (8). From (5) and (6) we obtain:

$$\alpha_6[M^-][NO^+] = (k_1[N_2] + k_2[NO])[O_2^+]; \qquad (9)$$

$$N = \frac{\xi S}{k_4[O_2] + k_5[NO]} \qquad (10)$$

We can then write, after some manipulation:

$$\frac{d[NO]}{dt} = 2S \left\{ \frac{1}{1 + \frac{k_2[NO]}{k_1[N_2]}} + \xi \left( \frac{1}{1 + \frac{k_5[NO]}{k_4[O_2]}} - \frac{1}{2} \right) \right\} \qquad (11)$$

Equation (11) has been solved numerically for $[NO]$ for the two cases $\xi = 0.2$ and $\xi = 0$; using these results in Equation (4), we have computed decay frequencies for $O_2^+$ as a function of irradiation time. Figure 7 shows these computed decay frequencies, normalized to unit pressure for both values of $\xi$.

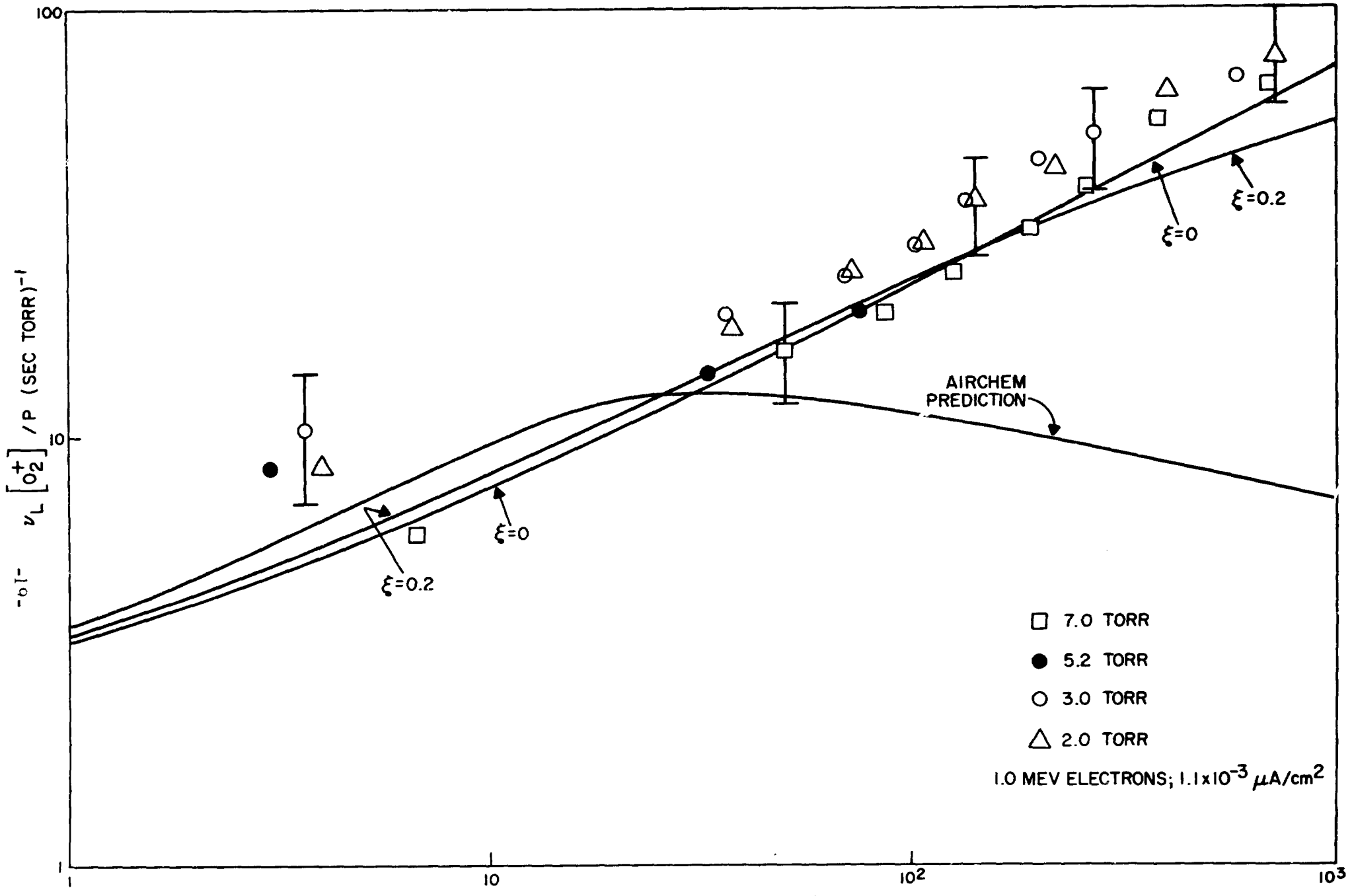


Figure 7. Comparison of Measurement and Prediction of the $O_2^+$ Decay Frequency per Unit Pressure as a Function of the Irradiation Time

Also shown in the figure are normalized decay frequencies computed from the AIRCHEM-code predictions of NO density made for 10.7 Torr [Niles, 1970]. The points displayed in the figure are the experimentally observed decay frequencies, also normalized to unit pressure. We have illustrated, by means of error bars on several of the points, an uncertainty of ± 25% which we attribute primarily to the uncertainty in absolute beam current density.

Several observations can be made immediately. First, the experimental data agree with the form and magnitude of the predictions from the simple model, to within the stated uncertainties. Second, the AIRCHEM prediction, which agrees with the simple model for the first 25 seconds of irradiation, shows a turnaround in the NO density, hence in the $O_2^+$ loss frequency at later times, which the data do not substantiate. The simple model contains no sink for NO; the AIRCHEM program does, of which the most important reaction under our conditions should be [Niles, 1970]:

$$NO + O_3 \longrightarrow NO_2 + O_2; \quad k_7 = 1.25 \times 10^{-14} cm^3/sec.$$

Since we do not yet monitor the neutral $O_3$ concentration, we have no way of knowing whether the discrepancy lies in our having an ozone density much smaller than the code predicts, or a reaction rate coefficient $k_7$ greatly in error, or whether still another sequence of chemical reactions not yet included in the code is needed to partially compensate for this removal mechanism. A better knowledge of the ionospheric sinks for NO would greatly enhance our understanding of in situ D-region chemistry.

Based on the data presented here, it is not possible to obtain a precise value for $\zeta$, the fraction of the ionization events which are dissociative. It appears from the data however, that $\zeta$ cannot be appreciably larger than 0.2.

Deviations from the predictions at early irradiation times may be attributed in part to $O_2^+$ recombination with all negative charge present. We can derive an upper limit to the recombination coefficient from these observed decay frequencies in the following way. The greatest observed early-time discrepancy is the 3 Torr point at 3-4 seconds, with a decay frequency about 5 $sec^{-1}$ in excess of the predictions of the simple model. If that frequency is due to recombination, we can write

$$\nu(O_2^+) = 5/\text{sec} \geq \alpha[M^-] = \sqrt{\alpha S},$$

since, in terms of the overall charge density, $S = \alpha [M^-]^2$. This yields as an upper limit

$$\alpha_3(O_2^+, M^-) \leq 1.4 \times 10^{-7} \text{ cm}^3/\text{sec}.$$

This contribution of 5 $sec^{-1}$ to the $O_2^+$ decay frequency is also small enough relative to the uncertainties in the measured absolute decay frequencies to justify its neglect in the development of Equation (8) above.

## VI. Effects of $H_2O$ on Ion Chemistry

### A. Introduction

Recent *in situ* measurements [Narcisi, 1967] have shown that water cluster ions, of the form $H_3O^+ \cdot n(H_2O)$, dominate the positive-ion spectrum in the D region of the ionosphere. Between 60 and 82 km, the cluster ion of mass 37 amu (n=1) is present in greatest abundance, with 19 amu (n=0) and 55 amu (n=2) also present, but in smaller concentrations. $NO^+$ is also present, but in lower concentrations than the 37-amu ion.

Stimulated by these observations and their potential significance to the physics of the ionosphere, we undertook a series of experiments to determine the effects of the addition of $H_2O$ to the airlike $N_2:O_2$ mixture spectra described in the previous section. We were particularly anxious to corroborate the ion identifications, to determine the $H_2O$ concentrations required for these ions to dominate the positive-ion spectra, and to determine the chemistry leading to the formation of this sequence of ions. Although the $H_2O$ concentrations used in the experiments are somewhat lower than those encountered in the atmosphere, it will be seen that the results span the interesting region over which the water-cluster ions change from minority status to dominance in the positive-ion spectra.

The $H_2O$ used in these experiments comes from two sources, the gas itself and the walls of the reaction chamber. $N_2:O_2$ mixtures with dew points of -100° F and -120° F (6.0 and 0.6 ppm $H_2O$, respectively) were used in the measurements. The chamber is periodically baked to produce base pressures in the low $10^{-8}$ Torr range prior to gas filling. After several experiments with the wetter of the two gases, occluded water on the chamber walls raises the ultimate pressure which

the system can attain. The water content of the gas which is quoted in the experiments below includes an estimate of this wall contribution, obtained from the measured outgassing rate of the chamber prior to filling.

## B. Experimental Results

Two types of measurements have been made on the air samples, mass scans at some definite time in the irradiation history of the gas, and ion decay measurements in the afterglow of a pulse of the 1-MeV electron radiation. Mass scans provide identification and an indication of the relative amount of each ion present at that time; the afterglow decays yield information on the loss processes for each ion. Because of the diffusive sampling in the mass spectrometer, ion decay rates observed in the spectrometer are not necessarily the ion decay rates in the chamber. We therefore use the relationship between ion densities, loss frequencies, and detected ion currents expressed by Equation (1).

Figure 8 is a summary of the positive-ion spectra observed during continuous irradiation of the airlike mixture at a pressure of 5 Torr as a function of the estimated $H_2O$ concentration. Results obtained at other pressures between 1 and 10 Torr do not differ in essentials. Before the spectra are recorded, the gas is irradiated for about an hour, to allow a quasi-equilibrium in the ionic and neutral chemistry to be reached. The spectra in the figure are normalized to equal values of the sum of the $NO^+$ and $NO^+ \cdot H_2O$ currents; this normalization permits certain trends in the ion chemistry to become apparent. (It should be remembered, however, that a more realistic normalization would be to equal total ion density, independent

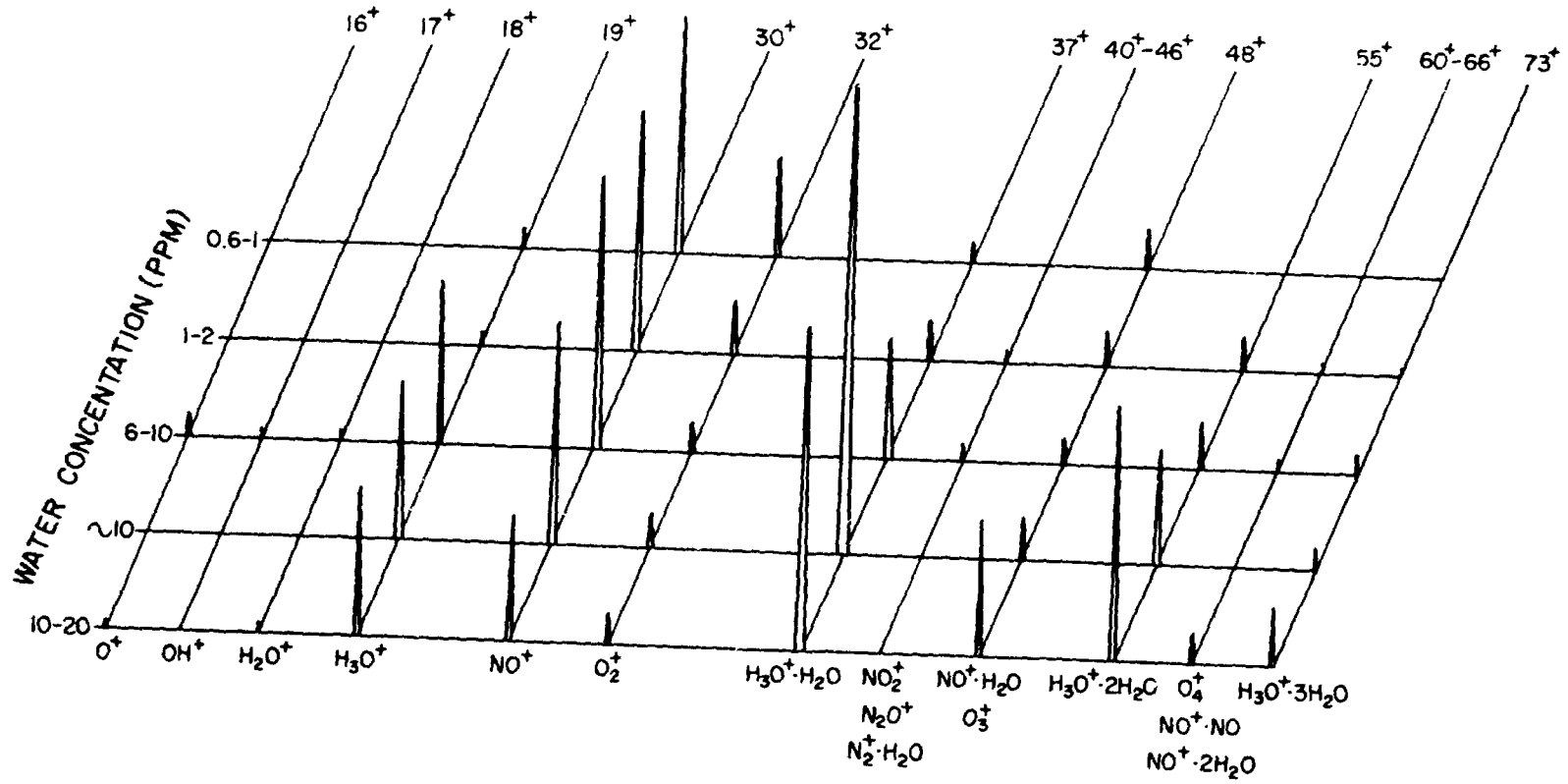


Figure 8. Summary of Positive-Ion Spectra in Airlike $N_2$:$O_2$ Mixtures as a Function of $H_2O$ Concentration

of $H_2O$ concentration.) From the figure, the water-cluster ions and $NO^+$ can be seen to dominate the spectrum, with a shift from $NO^+$ to the water ions as the $H_2O$ concentration is increased. The 37-amu ion dominates the spectrum for $H_2O \gtrsim 10$ppm as it does in the D region, although it remains comparable with $19^+$ throughout the entire range. The relative abundance of the higher molecular-weight cluster ions (55 and 73 amu) increases rapidly with increasing $H_2O$ concentration. For 20 ppm $H_2O$, $55^+$ is larger than $19^+$, although not as large as $37^+$.

We observe $NO^+ \cdot H_2O$ in some abundance, as well as a peak due to $H_3O^+ \cdot OH$ (36amu) on the side of the $37^+$ peak. Unfortunately, the poor signal-to-noise ratio requires operation of the monopole at low resolution to improve transmission (c.f. Appendix I); in particular, it would not be possible to observe a small $54^+$ ion on the side of the $55^+$ peak.

$O_2^+$ currents decrease with increasing $H_2O$ concentration relative to the other ions. This has important implications regarding the mechanism of the water-clustering sequence, as will be seen below.

Figure 9 shows the negative-ion spectrum obtained with $H_2O$ concentration somewhat greater than 10 ppm. The most important effect of increased water at these levels is the enhancement of the $NO_3^- \cdot H_2O$ peak at 80 amu; this peak is also observed in situ in the rocket measurements.

Four sets of afterglow measurements have been taken; they are illustrated in Figure 10. Both because of the poor signal-to-noise ratio of these afterglow decays and because of the complexity of the chemistry processes which produce and remove a given species, the conclusions drawn from these afterglows must be considered preliminary.

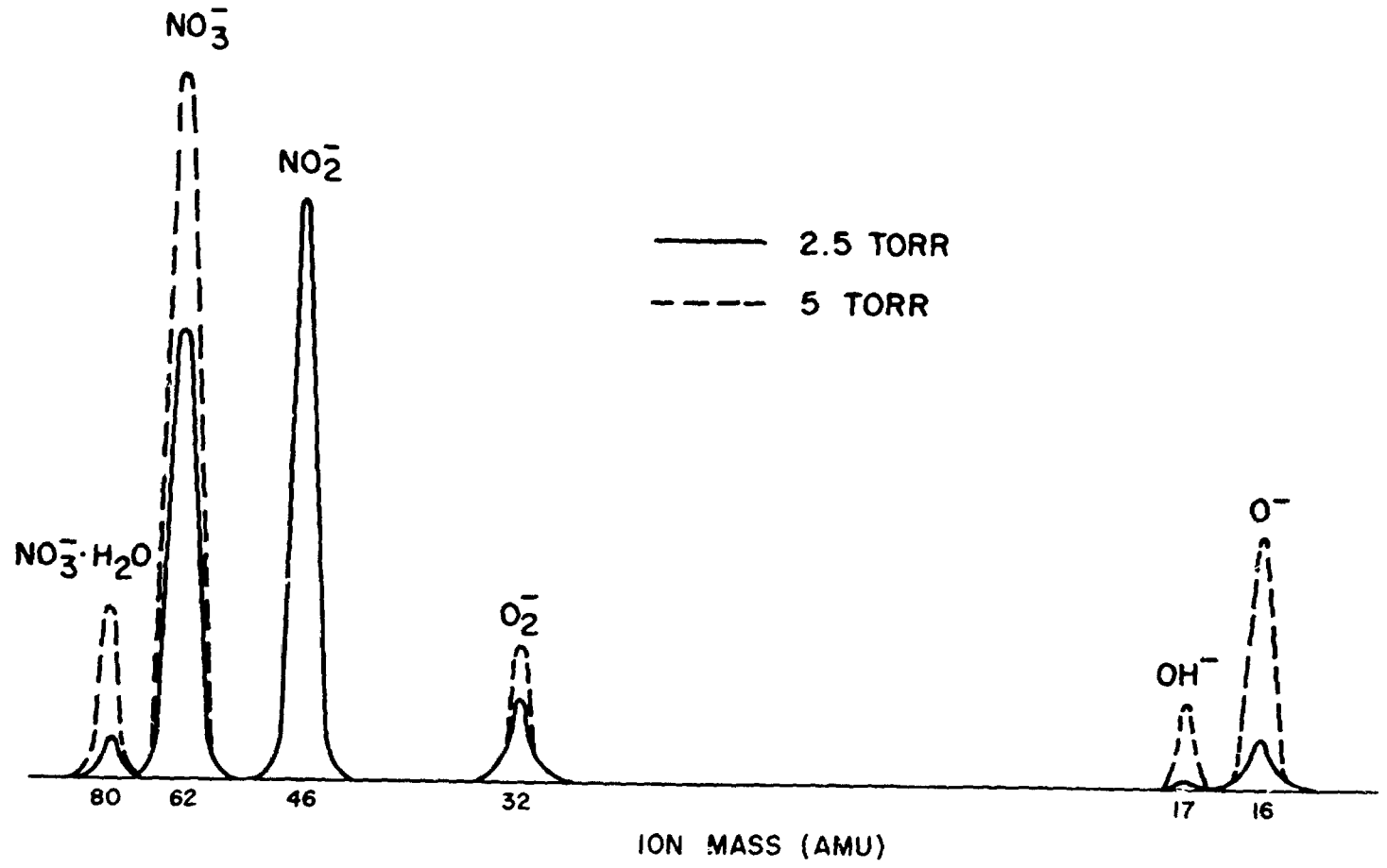


Figure 9. Quasi- Equilibrium Negative- Ion Spectra in Airlike $N_2$:$O_2$ after Prolonged Irradiation

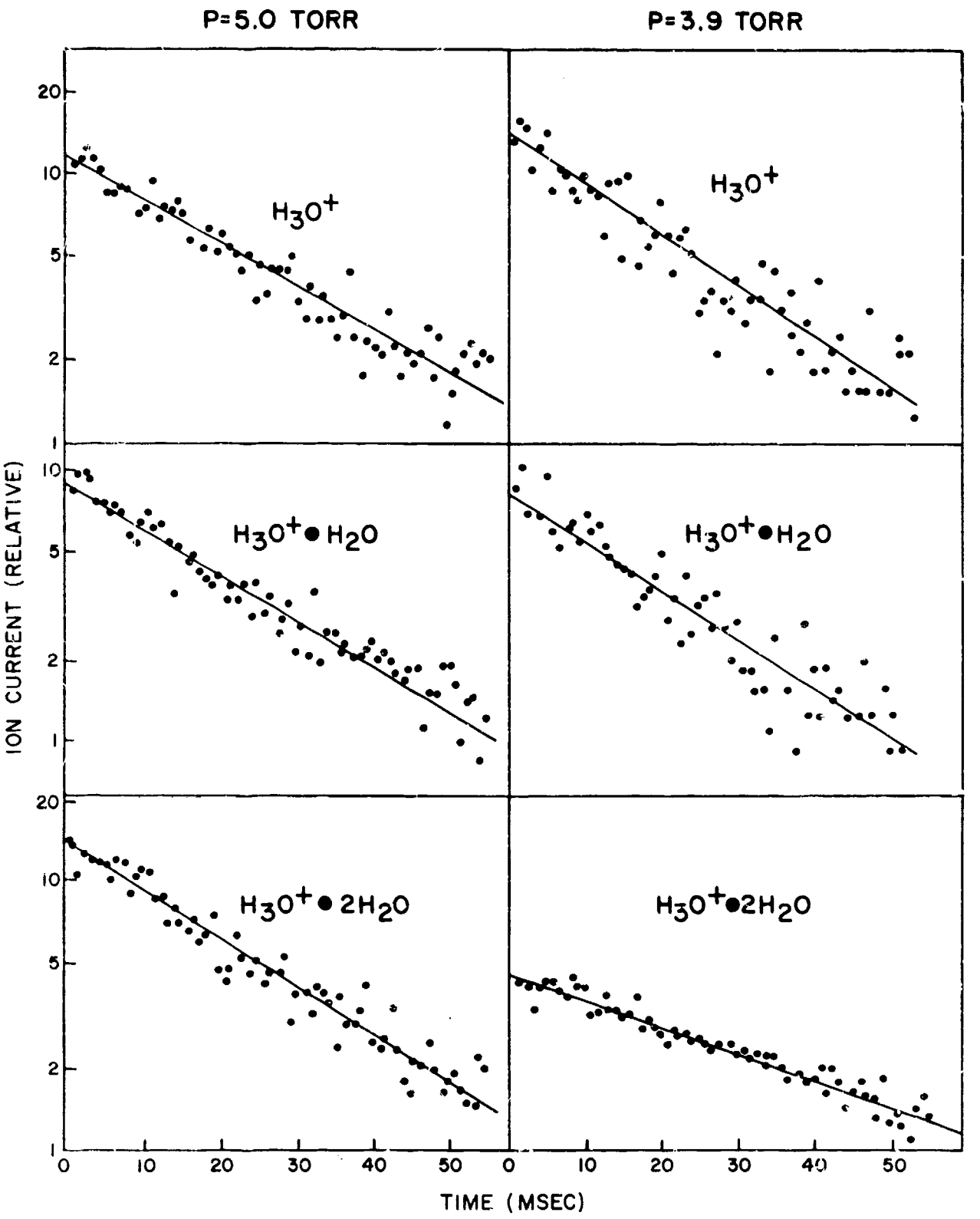


Figure 10. Afterglow Decays of the Cluster Ions $H_3O^+ \cdot nH_2O$ (n = 0, 1, 2)

From the afterglow measurements in $N_2$:$O_2$ mixtures containing 6-to 10-ppm $H_2O$, the cluster ions are seen to have nearly exponential decays. Exponential decays are characteristic of first-order chemical processes; in our experiments, in which $H_2O$ and total neutral molecule densities are time-invariant, a three-body hydration process such as

$$A^+ + H_2O + M \longrightarrow A^+ \cdot H_2O + M$$

appears as a quasi-first order reaction, and yields an exponential decay.

C. Water-Cluster Modelling

In the absence of large amounts of $O_2$, $H_2O^+$ reacts with $H_2O$ to form $H_3O^+$, the first member of the dominant ionospheric cluster-ion sequence $H_3O^+ \cdot nH_2O$.

$H_2O^+$ rapidly charge-exchanges with $O_2$, however, so another mechanism must be invoked to explain the formation of the sequence in the ionosphere. One such mechanism has been proposed recently by Fehsenfeld and Ferguson [1969]. The process begins with the hydration of a primary ion which we denote by $P^+$:

$$P^+ + H_2O + M \longrightarrow P^+ \cdot (H_2O) + M . \qquad (12)$$

(The large observed ionospheric concentration of cluster ions requires that $P^+$ be a majority-ion species.) Dimer ions of the form $P^+ \cdot P$, where P can be $O_2$, $N_2$, or NO, have available a more direct two-body hydration process:

$$P^+ \cdot P + H_2O \longrightarrow P^+ \cdot (H_2O) + P . \qquad (12')$$

The hydrated ion undergoes further hydration until, for some value of n, the reaction

$$P^+ \cdot n(H_2O) + H_2O \longrightarrow H_3O^+ \cdot (n-1)(H_2O) + P + OH \quad (13)$$

becomes exothermic. The hydrated cluster ion in (13) can continue to add (or subtract) water molecules through reversible reactions of the form

$$H_3O^+ \cdot (n-1)H_2O + H_2O + M \rightleftarrows H_3O^+ \cdot nH_2O + M . \quad (14)$$

If the positive ion $P^+$ in (12) is $O_2^+$, then reaction (13) becomes endothermic for n=1, directly producing $H_3O^+$(19amu); for $P^+=NO^+$, n=3 [Lineberger & Puckett, 1969], so that the smallest cluster ion directly produced from $NO^+$ has a mass of 55 amu. To complicate the picture, there is a competing reaction for $O_2^+ \cdot H_2O$:

$$O_2^+ \cdot H_2O + H_2O \longrightarrow H_3O^+ . OH + O_2 , \quad (15)$$

The complex ion thus formed may then react with $H_2O$,

$$H_3O^+ \cdot OH + H_2O \longrightarrow H_3O^+ . H_2O + OH \quad (16)$$

to produce the $37^+$ion, or in a three-body reaction with $O_2$ ,

$$H_3O^+ \cdot OH + O_2 + M \longrightarrow H_3O^+ \cdot OH \cdot O_2 + M , \quad (17)$$

which is then followed by the reactions

$$H_3O^+ \cdot OH \cdot O_2 + H_2O \longrightarrow H_3O^+ \cdot OH \cdot H_2O + O_2 \qquad (18)$$

$$H_3O+ \cdot OH \cdot H_2O + H_2O \longrightarrow H_3O^+ \cdot 2H_2O + OH \qquad (19)$$

to produce 55+. A summary of the intermediate and product ions which this scheme predicts that we might see in "wet" air is given in Table I below.

TABLE I

| ION | MASS | REACTION NO. |
|---|---|---|
| $N_2^+ \cdot (H_2O)$ | 46 | (12) |
| $O_2^+ \cdot (H_2O)$ | 50 | (12), (12') |
| $NO^+ \cdot (H_2O)$ | 48 | (12) |
| $H_3O^+$ | 19 | (13) ($P^+ = O_2^+$) |
| $H_3O^+ \cdot OH$ | 36 | (16) |
| $H_3O^+ \cdot OH \cdot O_2$ | 68 | (17) |
| $H_3O^+ \cdot OH \cdot H_2O$ | 54 | (18) |
| $H_3O^+ \cdot (H_2O)_2$ | 55 | (19), (13)($P^+ = O_2^+$) |
| $H_3O^+ \cdot (H_2O)_n$ | 37,55,73, etc. | (14) |
| $H_3O^+ \cdot H_2O$ | 37 | (16) |

## D. Comparison with Available Data

Of the ions listed in Table I, it is interesting to note that we observe, in addition to the hydrated complex ions themselves at masses 19, 37, 55, and 73, the intermediate ions of mass 48 ($NO^+ \cdot H_2O$) and 36 ($H_3O^+ \cdot OH$). The other intermediate ions listed in the table, even if present in the amounts predicted by the theory, could not be resolved by the apparatus in its present operating mode, in view of the small expected magnitudes of these ions relative to the large peaks at adjacent mass numbers. Thus, the limited data available from the ion identifications alone do not conflict with the Fehsenfeld-Ferguson model presented above.

We observe relatively large $O_2^+$ currents in our ion-spectrum observations, and see no discernible $O_4^+$ peak. If we accept the spectrometer identifications as representative of the ionic composition of the irradiated gas in the chamber, then the observed rapid decrease of $O_2^+$ with increasing water concentration is explained by Equation (12). If the observed $O_2^+$ peak is the result of both $O_2^+$ in the chamber and $O_4^+$ from the chamber which is broken up in the spectrometer sampling process, for example, then the comment is still valid, but reaction (12') must also be invoked. Although $NO^+$ also decreases upon the addition of more water, due both to direct $NO^+$- $H_2O$ chemistry and to the loss of $O_2^+$ which produces $NO^+$ by charge exchange, quantitative considerations show that the $O_2^+$ decrease is much greater than that expected for $NO^+$ [Niles, 1970].

In the reaction chamber, the afterglow behavior of a water-cluster ion is given by

$$\frac{d[H_3O^+ \cdot nH_2O]}{dt} = (k_8[H_2O][M] + \alpha_n[M^-][H_3O^+ \cdot nH_2O] + k_9[H_3O^+ \cdot (n+1)H_2O][H_2O][M] \quad (20)$$

$k_8$ is the three-body hydration reaction rate, $k_9$ the reverse rate:

$$H_3O^+ \cdot nH_2O + H_2O + M \underset{k_9}{\overset{k_8}{\rightleftharpoons}} H_3O^+ \cdot (n+1)H_2O + M. \quad (21)$$

The ionic recombination coefficient $\alpha_n$ is an "effective", time dependent coefficient because of the changing composition of the negative-ion spectrum during the afterglow. Only if the hydration reaction ($k_8$) dominates the afterglow will the ion decay be describable by a single exponential; from Equation (1), only for such decays can the observed ion-current decay rate be simply related to the true ion loss frequency.

We have analyzed the four observed afterglow decays of the $H_3O^+$ ion (19amu) under the assumption that they are exponential and that they represent reaction $k_8$. The values obtained from the individual runs are 2.1, 2.3, 2.8, and 4.0 x $10^{-28}cm^6/sec.$, respectively. This yields an average value for $k_8$ of 2.8 x $10^{-28}cm^6/sec$, which should be compared with the approximate value of 1.0 x $10^{-27}cm^6/sec$ measured by Burt [1968], and used by Ferguson and Fehsenfeld [1969] for their ionospheric modelling studies. Because of the unknown amount of reverse reaction in (21), our value for $k_8$ is in the nature of a lower bound.

Similar analysis has been made for the ($H_3O^+ \cdot H_2O$) ion (37 amu). Here too the afterglows appear exponential, and yield an average reaction rate of 3.6 x $10^{-28}cm^6/sec$.

For $H_3O^+ \cdot 2H_2O$ (55 amu) which decays more slowly than either $19^+$ or $37^+$, the afterglow ion currents are not exponential; this is due at least in part to the effects of continued production of $55^+$ in the afterglow, but may also indicate that some of these ions disappear by recombination with negative ions. The accuracy of the reaction-rate estimates given above is on the order of a factor of 2. This is due primarily to the uncertainty of the actual concentration of water in the vapor phase, as explained earlier. Nonetheless, the measured decay rates are sufficiently close to those measured by other workers to be hightly suggestive that the modelling picture outlined by Fehsenfeld and Ferguson and described in the previous chapter is essentially correct, at least for our experimental conditions.

## VII. Summary

We have studied the positive and negative ion spectra resulting from the irradiation of air by high-energy electrons. Megavolt electrons with a flux density of the order of $1 \times 10^{-3}\mu$ A/cm$^2$ uniformly irradiate a 700$\ell$ gas-filled reaction chamber; the irradiation produces a weak plasma with an average density of about $10^8$ ions/cm$^3$ at total gas pressures of from 1 to 10 Torr at 300°K. When the electron beam first irradiates the gas, the positive atomic and molecular ions $O^+$, $O_2^+$, $N^+$, and $N_2^+$ are produced, along with secondary electrons. The positive ions rapidly charge exchange with $O_2$ in irradiation times well within 1 second to reduce the positive ion spectrum to a single observed species, $O_2^+$; three-body attachment of the secondary electrons results in a single observable negative ion, $O_2^-$, also within the first second of irradiation. As the irradiation continues, chemical reactions change this simple ion spectrum: $O_2^+$ and $O_2^-$ decrease, and new ions such as $NO^+$, $NO_2^-$, $NO_3^-$, and $O_3^-$ appear. After long irradiation (more than 10 minutes), the $NO^+$ ion dominates the positive ion spectrum in dry air (<1 ppm water), and hydrated cluster ions of the form $H_3O^+ \cdot nH_2O$, along with $NO^+$, dominate the positive ion spectrum in wet air. The dominant negative ions at these long irradiation times are $NO_2^-$ and $NO_3^-$, in both wet and dry air.

The initial decrease in $O_2^+$ density is due to charge exchange with NO which is produced by reactions of electron-beam generated N and $O_2^+$ on $O_2$ and N respectively. This process has been studies in some detail; the $O_2^+$ loss frequency has been shown to vary with irradiation time t as

$$\nu_L(O_2^+) = (85 \pm 20)\ p\sqrt{it}\ \text{sec}^{-1} \quad (t \geq 5 \text{ sec.})$$

From the analysis of the chemistry involved in this process, we find that the reaction rate for the charge rearrangement reaction

$$O_2^+ + N_2 \xrightarrow{k_1} NO^+ + NO$$

is $k_1=(1.0\pm0.25) \times 10^{-16}cm^3/sec$. At earlier irradiation times, of the order of 1 sec, $O_2^+$ is lost by recombination with the available negative ion, primarily $O_2^-$; an upper limit for the recombination coefficient of $1.4 \times 10^{-7}cm^3/sec$ has been deduced from the afterglow decay data.

We can summarize the results of the water-chemistry studies after prolonged irradiation by the following statements:

1. Water-cluster ions of the form $H_3O^+ \cdot nH_2O$ (n=0, 1,2) dominate the positive-ion spectrum in weakly-ionized air at 300°K, at pressures between 1 and 10 Torr, and for $H_2O$ concentrations on the order of 10 ppm or more. This agrees with the in situ results obtained in the D region, although at different temperatures and pressures, and suggests an ambient $H_2O$ concentration there too of the order of 10 ppm or more.

2. Our experimental results are compatible with the hydration sequence proposed by Fehsenfeld and Ferguson. We observe $NO^+ \cdot H_2O$ and $H_3O^+ \cdot OH$, in addition to the dominant cluster ions. We also note that $O_2^+$ (or perhaps $O_4^+$ ) is more strongly removed by water than is $NO^+$.

3. From afterglow measurements we observe that $H_3O^+$ and $H_3O^+ \cdot H_2O$ appear to be lost in quasi-first order hydration reactions, with effective rate coefficients $2.8 \times 10^{-28} cm^6/sec$ and $3.6 \times 10^{-28} cm^6/sec$, respectively. The effective rate coefficients are accurate to within about a factor of 2. The presence of reverse reactions not accounted for in the analysis may have reduced the effective removal rates for these ions below that due to the hydration loss itself.

4. The negative-ion spectrum is essentially unchanged by the presence of water at least up to concentrations of 20 ppm, beyond a small increase in the ion peak at 80 amu ($NO_3^- \cdot H_2O$). The dominant negative ions still recombine with $NO^+$, even in the presence of the cluster ion.

## APPENDIX I - Ion Sampling Considerations

Mass spectrometer ion studies are usually performed adjacent to small chambers filled with low-pressure gas, in which the ion densities are essentially diffusion controlled. Under those conditions the ion current which diffuses to the walls and is sampled in the mass spectrometer is directly proportional to the central ion density. In our large chamber the vast majority of the ions interact by volume processes, and diffusion is only important within a few centimeters from the walls. We have found the following simple physical argument adequate to describe the relationship between central density and wall current appropriate to this situation.

Consider the one-dimensional plasma shown in Figure 11. The ion density $n_c$ in the central region is controlled by volume production at the rate P, and by volume loss at an effective removal frequency $\nu_L \equiv dn_c/dt$. Because of the spatial uniformity of our electron-beam source term, the central ion density $n_c = P/\nu_L$ can be represented by the horizontal line shown in the figure. But diffusion must be important near the walls, and the ion density must in fact vanish at the walls themselves. We, therefore, approximate the ion density profile by a trapezoid; the slopes of the sides are chosen so that at point A the loss rate due to diffusion is equal to that due to the volume process, that is:

$$D\left(\frac{\partial^2 n}{\partial x^2}\right)_A = \nu_L \; n_c. \qquad (A\text{-}1)$$

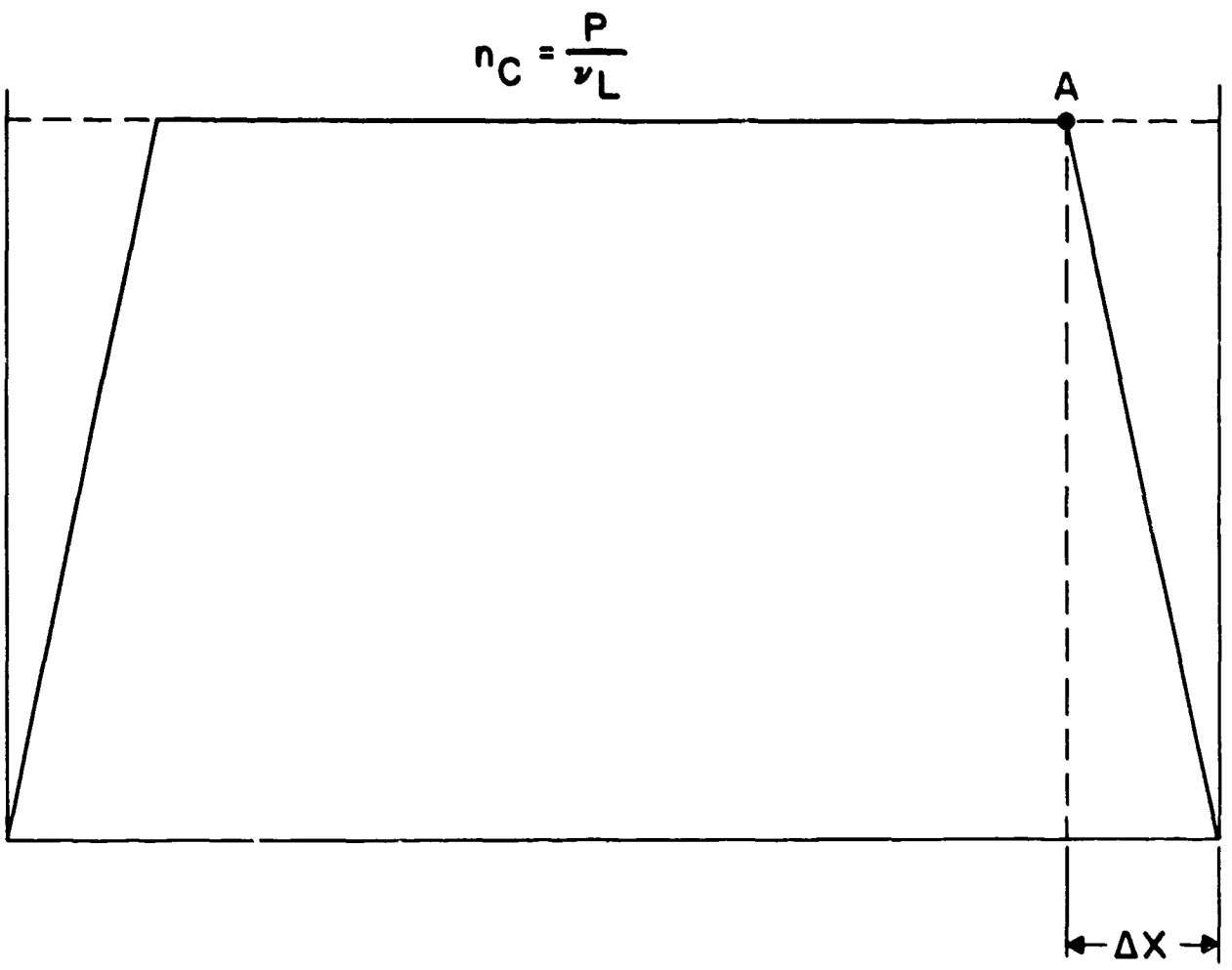


Figure 11. Spatial Profile of Ion Density Assumed for Sampling Theory

We can approximate the spatial derivatives by

$$\left(\frac{\partial n}{\partial x}\right)_A \simeq \frac{n_c}{\Delta x} ; \quad \left(\frac{\partial^2 n}{\partial x^2}\right)_A \simeq \frac{n_c}{(\Delta x)^2} . \qquad \text{(A-2)}$$

Thus (A-1) is satisfied, to this approximation, by locating point A a distance $\Delta x = (D/\nu_L)^{1/2}$ from the wall. So defined, $\Delta x$ is a measure of the penetration of diffusion effects into the volume of the chamber. The diffusion-current density to the walls is then given by

$$\Gamma_{wall} \approx D \frac{n_c}{\Delta x} = \sqrt{D\nu_L}\, n_c \ (\text{cm}^2 \text{ sec})^{-1} . \qquad \text{(A-3)}$$

Some numerical considerations are instructive at this point. Under typical operating conditions in our chamber at 1 Torr, we find $n_c \approx 10^8/\text{cm}^3$, $D \approx 50$ cm$^2$/sec, and $\nu_L \approx 20$/sec. (see Figure 4). For these conditions, $\Delta x \approx 1.5$ cm, which is certainly small compared with any geometrical dimensions encountered in the experiment. With diffusion effects thus confined to a thin layer near the walls, we can expect the particle density gradients in our three-dimensional experiment to be normal to the chamber walls, thus permitting the direct application of the one-dimensional theoretical treatment above to the experiment.

For these same numerical values, we obtain a wall current density of the order of $3 \times 10^4$ ions/cm$^2$sec. The mass-spectrometer aperture has an area of $3 \times 10^{-3}$ cm$^2$, so the total particle flux through the aperture is on the order of $10^7$ ions/sec , corresponding to a current on the order of $10^{-12}$A at the input to the spectrometer. We have estimated the transmission of the spectrometer system at low resolution to be on the order of 1%, and to decrease significantly as the resolution is increased;

thus maximum ion currents on the order of $10^5$/ions/sec, or $10^{-14}$A, can be expected. For minority species, or in the afterglow, even smaller currents are obtained. This illustrates the need for pulse counting techniques, and for operation of the spectrometer at low resolution.

The theory presented above predicts a reasonable and dimensionally correct variation of ion wall current with physical parameters. Thus, as the ion frequency is increased, we can expect $\Delta x$ to decrease, since the diffusion then competes less effectively against the volume loss process. Quasi-first order processes, for which $\nu_L$ is not a function of the densities of beam-generated species, are characterized by $\Gamma$(wall) which vary directly as the true central density; in particular, the observation of an exponential decay in the ion current implies an exponential decay of the central ion density with the same time constant. For recombination between a single species each of positive and negative ions, $\nu_L$ is directly proportional to the central ion density ($\nu_L = \alpha_n n_c$), so $\Gamma$(wall) varies as $n_c^{3/2}$. We have in fact compared this latter case with the relationship computed numerically from the theory of Gray and Kerr [1962] for recombination-diffusion afterglows in an infinite cylindrical geometry; the two treatments predict the same dependence of $\Gamma$(wall)/$n_c$ on physical parameters, and differ only by a multiplicative factor of the order of 2.

Another case for which comparison is relatively simple is the steady-state one-dimensional plasma with a spatially uniform source term, and both diffusive loss and a linear volume loss of ions:

$$P = \nu_L n + D \frac{dn}{dx} \qquad (A-4)$$

The solution of (A-4) for the boundary conditions n=0 at the walls yields a diffusive wall current, in the

limit of small diffusion, identical to that given in Equation A-3.

## REFERENCES


Burt, J.A., Thesis, York University, Toronto (1968).

Dalgarno, A., Space Sci. 7, 849 (1967).

Eisner, P.N. and Hirsh, M.N., "Ion Recombination Coefficients Measured in a Simulated Disturbed Ionosphere", paper delivered at The Symposium on Physics and Chemistry of the Upper Atmosphere, Philadelphia (1970), (in preparation for publication).

Fehsenfeld, F. C. and Ferguson, E. E., J. Geophysical Research 74, 2217 (1969) and 74, 5743 (1969).

Gray, E. P. and Kerr, D. E., Ann Phys. (N.Y.) 17, 276 (1962).

Hirsh, M. N., Eisner, P. N. and Slevin, J. A., Rev. Sci. Instr. 39, 1547 (1968).

Hirsh, M. N., Eisner, P. N., and Slevin, J. A., Phys. Rev. 188, 175 (1969).

Hirsh, M. N., E. Poss, and P. N. Eisner, Phys. Rev. A, 1, 1615 (1970).

Keneshea, T. J., Research Report AFCRL-67-0221, April 1967 (unpublished).

Lineberger, W. C., and L. J. Puckett, Phys. Rev. 186, 116 (1969).

Narcisi, R. S., Space Research VII, 186 (1967).

Niles, F. E., J. Chem. Phys. 52, 408 (1970).

Unclassified
Security Classification

## DOCUMENT CONTROL DATA - R & D

*(Security classification of title, body of abstract and indexing annotation must be entered when the overall report is classified)*

1. ORIGINATING ACTIVITY *(Corporate author)*
The Dewey Electronics Corporation
11 Park Place
Paramus, N. J. 07652

2a. REPORT SECURITY CLASSIFICATION
Unclassified

2b. GROUP

3. REPORT TITLE
Further Laboratory Studies of the Perturbed Upper Atmosphere

4. DESCRIPTIVE NOTES *(Type of report and inclusive dates)*
Final Report, 1 July 1969 - 30 June 1970

5. AUTHOR(S) *(First name, middle initial, last name)*
Merle N. Hirsh
Philip N. Eisner

| 6. REPORT DATE | 7a. TOTAL NO. OF PAGES | 7b. NO. OF REFS |
|---|---|---|
| 15 July 1970 | 42 | 12 |

8a. CONTRACT OR GRANT NO. ~~DASA01-67-C-0020-P001~~ DASA-01-70-C-0032
b. PROJECT NO. NWER XAXH
c. Task & Subtask C010
d. Work Unit 06

9a. ORIGINATOR'S REPORT NUMBER(S)
R-251

9b. OTHER REPORT NO(S) *(Any other numbers that may be assigned this report)*
DASA 2536

10. DISTRIBUTION STATEMENT
Each transmittal of this document outside the agencies of the U.S. Government must have prior approval of the Director, Defense Atomic Support Agency, Washington, D.C. 20305

11. SUPPLEMENTARY NOTES

12. SPONSORING MILITARY ACTIVITY
Director
Defense Atomic Support Agency
Washington, D.C. 20305

13. ABSTRACT

Laboratory studies have been made of the positive and negative ions resulting from the irradiation of airlike $N_2$:$O_2$ mixtures at total pressures between 1 and 8 Torr by megavolt electrons. For gas mixtures containing less than 1 ppm $H_2O$, only $O_2^+$ and $O_2^-$ are observed at the onset of irradiation; as the electron bombardment continues, these ions interact woth beam-generated minority species to produce an ion spectrum eventually dominated by $NO^+$, $NO_2^+$, and $NO_3^+$. Quantitative studies of the removal of $O_2^+$ by charge-exchange with beam-generated NO yield for the dominant NO-producing mechanism the reaction

$$O_2^+ + N_2 \rightarrow NO^+ + NO,$$

with the rate coefficient $K=(1.0 \pm 0.25) \times 10^{-16}$ $cm^3$/sec. From the

(Continued - See Atachment "A")

| 14. KEY WORDS | LINK A | | LINK B | | LINK C | |
|---|---|---|---|---|---|---|
| | ROLE | WT | ROLE | WT | ROLE | WT |
| Positive and Negative Ions<br>Radiation Chemistry<br>Disturbed Ionosphere<br>Hydrated Cluster Ions<br>Nitric Oxide<br>Relativistic Electrons | | | | | | |

ATTACHMENT "A" TO DD FORM 1473

13. Abstract - Continued

initial $O_2^+$ decays, an upper limit of 1.4 X $10^{-7}$ $cm^3$/sec is found to the coefficient for two-body ionic recombination of $O_2^+$ and $O_2^-$. If $H_2O$ concentrations between 5 and 20 ppm are added to the gas, the positive ion spectrum observed after long irradiation is dominated by complex ions of the form $H_3O^+ . n\ H_2O$ (n=0, 1, 2, ...), in agreement with in situ observations in the D region. In the radiation afterglow, $H_3O^+$ and $H_3O^+ . H_2O$ are lost by first-order reactions with apparent rate coefficients of 2.8 x $10^{-28}$ $cm^6$/sec, respectively, to within a factor of 2. Except for a small increase in the $NO_3^- . H_2O$ peak, the negative ion spectrum is essentially unchanged by concentration of up to 20 ppm $H_2O$. (U)

**Defense Threat Reduction Agency**
45045 Aviation Drive
Dulles, VA 20166-7517

CPWC/TRC November 3, 1999

MEMORANDUM FOR DEFENSE TECHNICAL INFORMATION CENTER
ATTN: OCQ/MR WILLIAM BUSH

SUBJECT: DOCUMENT CHANGES

The Defense Threat Reduction Agency Security Office has performed a classification/distribution statement review for the following documents:

DASA-2519-1, AD-873313, STATEMENT A
DASA-2536, AD-876697, STATEMENT A
DASA-2519-2, AD-874891, STATEMENT A
DASA-2156, AD-844800, STATEMENT A
DASA-2083, AD-834874, STATEMENT A
DASA-1801, AD-487455, STATEMENT A
POR-4067, AD-488079, STATEMENT C, ADMINISTRATIVE/OPERATIONAL USE
DASA-2228-1, AD-851256, ~~STATEMENT~~ C, No Target only chged from ST A to adm/oper. ADMINISTRATIVE/OPERATIONAL USE
RAND-RM-2076, AD-150693, STATEMENT D, ADMINISTRATIVE/OPERATIONAL USE
AD-089546, STATEMENT A, ADMINISTRATIVE/OPERATIONAL USE * ST-A Jan'65
DASA-1847, AD-379061, UNCLASSIFIED, STATEMENT C, ADMINISTRATIVE/OPERATIONAL USE ~~NOT APPLICABLE~~ C
~~RAND-RM-4812-PR~~, ELEMENTS OF A FUTURE BALLISTIC MISSILE TEST PROGRAM, UNCLASSIFIED, STATEMENT C, ADMINISTRATIVE/OPERATIONAL USE 370168 Conf
Authority to Declassify

If you have any questions, please call me at 703-325-1034.

Leave ST-A
Gen A. Jarrett
23 Nov 99

Ardith Jarrett

ARDITH JARRETT
Chief, Technical Resource Center